Published as: *ACS Nano*. 2009 November 24; 3(11): 3719–3729.

Layer-by-Layer Assembled Multilayer Films for Transcutaneous Drug and Vaccine Delivery

Xingfang Su[1,†], **Byeong-Su Kim**[2,†,◇], **Sara R. Kim**[2], **Paula T. Hammond**[2,3,*], and **Darrell J. Irvine**[1,3,4,5,*]

[1] Department of Material Science and Engineering, Massachusetts Institute of Technology, 77 Massachusetts Avenue, Cambridge, MA 02139

[2] Department of Chemical Engineering, Massachusetts Institute of Technology, 77 Massachusetts Avenue, Cambridge, MA 02139

[3] Koch Institute for Integrative Cancer Research, Massachusetts Institute of Technology, 77 Massachusetts Avenue, Cambridge, MA 02139

[4] Department of Biological Engineering, Massachusetts Institute of Technology, 77 Massachusetts Avenue, Cambridge, MA 02139

[5] Ragon Institute of MGH, MIT, and Harvard, Boston, MA 02114

[6] Howard Hughes Medical Institute, 4000 Jones Bridge Rd., Chevy Chase, MD 20815

Abstract

We describe protein- and oligonucleotide-loaded layer-by-layer (LbL)-assembled multiplayer films incorporating a hydrolytically degradable polymer for transcutaneous drug or vaccine delivery. Films were constructed based on electrostatic interactions between a cationic poly(β-amino ester) (denoted Poly-1) with a model protein antigen, ovalbumin (ova), and/or immunostimulatory CpG (Cytosine–phosphate diester—Guanine rich) DNA oligonucleotide adjuvant molecules. Linear growth of nanoscale Poly-1/ova bilayers was observed. Dried ova protein-loaded films rapidly deconstructed when rehydrated in saline solutions, releasing ova as non-aggregated/non-degraded protein, suggesting that the structure of biomolecules integrated into these multilayer films are preserved during release. Using confocal fluorescence microscopy and an *in vivo* murine ear skin model, we demonstrated delivery of ova from LbL films into barrier-disrupted skin, uptake of the protein by skin-resident antigen-presenting cells (Langerhans cells), and transport of the antigen to the skin-draining lymph nodes. Dual incorporation of ova and CpG oligonucleotides into the nanolayers of LbL films enabled dual release of the antigen and adjuvant with distinct kinetics for each component; ova was rapidly released while CpG was released in a relatively sustained manner. Applied as skin patches, these films delivered ova and CpG to Langerhans Cells in the skin. To our knowledge, this is the first demonstration of LbL films applied for the delivery of biomolecules into skin. This approach provides a new route for storage of vaccines and other immunotherapeutics in a solid-state thin film for subsequent delivery into the immunologically-rich milieu of the skin.

[*]Authors to whom correspondence should be addressed: hammond@mit.edu, djirvine@mit.edu.
[†]These authors contributed equally to this work
[◇]This author is now at School of Energy Engineering and School of NanoBio and Chemical Engineering, Ulsan National Institute of Science and Technology (UNIST), Korea

Supporting Information Available: Chemical structures of Poly-1 and Poly-2, ova loading at different pHs, non-reducing SDS-PAGE of ova released from films and histology sections of tape-stripped murine ears. This material is available free of charge via the Internet at http://pubs.acs.org.

Keywords

layer-by-layer; transcutaneous delivery; vaccine; polymer assembly; biodegradable

Polyelectrolyte multilayers have attracted much interest for their versatility, ease of preparation, and ability to conformally coat virtually any substrate.[1–6] Pioneering studies demonstrated that proteins could be assembled into such multilayers[7, 8] and retain their functionality,[9] stimulating a broad interest in potential biomedical applications of these materials.[3, 10] Further, the ability of multilayers to be built from biocompatible and bioresorbable polyelectrolytes has led to additional applications, including modification of cell adhesion on surfaces,[11] tissue- and skin-bonding films,[12] coatings directly applied to epithelial or endothelial cell layers in situ[13, 14], or even coatings on living single cells.[15–17]

In concert with a growing interest in applying multilayers to biomedical applications, erodible multilayers that deconstruct in aqueous conditions via disassembly and/or breakdown of the constituent polymers have begun to be explored as potential controlled release drug delivery films.[18–21] Drug-loaded degradable multilayers have been explored for the sustained release of small-molecule antibiotics, protein therapeutics, or plasmid DNA.[3, 7, 18, 19, 21–24] The mild aqueous conditions for encapsulating molecules into multilayer films preserves the bioactivity of fragile biomolecules such as proteins and nucleic acids.[21, 22, 25] By employing degradable polyelectrolytes as building blocks, the ability to tune the degradation kinetics of multilayer assemblies has been demonstrated and used to control the release kinetics of compounds embedded in these films.[20, 26] Applications envisioned for such drug-loaded films include antimicrobial- or anti-inflammatory coatings on implants and drug-releasing coatings for stents.[24, 27, 28]

Given the ability of multilayers to be conformally coated on a broad range of substrates, to load both small-molecule and macromolecular drugs, and to regulate the release of drugs over a period of hours to days, we became interested in the potential of these polyelectrolyte films in a new application area: transcutaneous drug delivery. Skin is an attractive site for non-invasive delivery of therapeutics, due to the ease of access to this organ and the ability of transcutaneous delivery to limit first-pass drug metabolism and alter the pharmacokinetics and pharmacodynamics of drugs.[29, 30] Epicutaneous immunization, the topical delivery of vaccine antigens into the epidermis or dermis of skin, offers the advantages of needle-free delivery while targeting an immune sentry-rich natural portal of pathogen entry.[31–33] We hypothesized that drug-loaded multilayers coated on the surface of a skin-adhesive patch or wound dressing could provide several attractive features for transcutaneous drug delivery: (i) Interactions of embedded proteins with the multilayer components might stabilize proteins against aggregation on drying, facilitating storage of protein therapeutics in a dry state; (ii) The concentration of a substantial cargo of drug into an ultrathin coating directly apposed to the surface of the skin would provide a strong diffusive driving force promoting penetration of drug cargos into the skin; (iii) multilayers could be designed to release multiple components and separately regulate the kinetics of release of individual drug components to optimize a therapeutic response; and (iv) the versatility of multilayer assembly would allow this concept to be implemented in a variety of transcutaneous delivery settings, including coatings of simple skin-adhesive patches, woven-fiber adhesive dressings, or microneedle arrays.

Here we report on studies testing each aspect of this hypothesis, in a model setting of protein-and DNA-loaded multilayer thin films coated on model skin patch substrates. We demonstrate that biodegradable multilayers can be loaded with a model protein antigen at doses physiologically relevant to vaccination, that dried multilayers release the embedded

protein in a monomeric, unaggregated form on rehydration and erosion of the films, and that model patch substrates coated with multilayers and applied to tape-stripped skin (a simple procedure often used to permeabilize the outer layers of the stratum corneum in transcutaneous vaccination studies[34–36]) rehydrate and dissolve *in situ*, releasing protein into the epidermis. Using a transgenic mouse model where epidermal antigen presenting cells (Langerhans cells) express green fluorescent protein (GFP)-tagged Major Histocompatibility Complex molecules, we demonstrate that protein antigen released from multilayer patches is acquired by these immune cells in the skin within hours of application of the film. Finally, we demonstrate the incorporation of multiple drug cargos in films, illustrated for the case of vaccine design by embedding a protein antigen together with an adjuvant molecule, single-stranded CpG DNA oligonucleotides. We show that antigen and adjuvant can be loaded together in decomposable multilayer coatings and released with distinct kinetics, as may be desirable for temporally controlling the induction of an immune response (or other therapeutic response). Using the murine skin model, we show that both vaccine components can be delivered to Langerhans cells in the epidermis from skin-applied multilayer films.

RESULTS AND DISCUSSION

To fabricate a PEM film capable of releasing macromolecular cargos into skin, we utilized polyelectrolytes belonging to the family of poly(β-amino esters), known to degrade hydrolytically under physiological conditions, focusing on two members of this family designated Poly-1 and Poly-2 (Figure 1 and Supporting Information, Figure S1).[37] The biocompatibility of Poly-1 has been established in earlier studies, and we have previously employed this polymer to fabricate LbL films with controlled erosion and tunable drug release profiles.[19, 22, 38] As a model protein cargo, we examined the assembly of multilayers containing ovalbumin (ova), a 45 KDa globular protein routinely used as a model vaccine antigen.[39–41]

We first prepared PEM films by alternating adsorption of Poly-1 and ova from aqueous buffers onto glass slides, utilizing electrostatic interactions between the protein and polymer to mediate assembly and monitoring protein incorporation via the absorbance of fluorophore-conjugated ova. Based on the p*I* of ova (~4.6) and the pK_a of Poly-1 (between 4.5 – 8), we tested film assembly at pH 5 –7, varying the pH of both Poly-1 and ova adsorption solutions (Figure S2).[37] As summarized in Figure 1b, film growth was approximately linear for deposition buffer pH values of 5/6 and 6/6 for Poly-1/ova bilayers. Maximal incorporation of ova was achieved by adsorbing both Poly-1 and ova at pH 6. For ova adsorption buffers at pH > 6, loading decreased, possibly due to decreasing charge density of Poly-1, which contains tertiary amine groups, at higher pH.[19] Measurement of the total amount of ova released from completely dissolved films showed that for films assembled at pH 6, 40-bilayer films carried 5 μg/cm^2 ova protein total (40-bilayer films are ca. 150 nm). In the context of vaccination, this order of dose/area is well within a meaningful range as antibody responses have been reported for transcutaneous antigen doses as low as 3 μg.[42–44]

When dried as-assembled (Poly-1/ova)$_n$ PEM films on glass were rehydrated in phosphate-buffered saline (PBS, pH 7.4), films prepared across all deposition conditions exhibited rapid protein release, as illustrated in Figure 1c. Characterization of (Poly-1/ova)$_{40}$ film thickness vs. time following rehydration revealed rapid dissolution of the films coinciding with protein release. These films fall apart significantly more rapidly than others assembled with other proteins or biopolymers[19, 21], and also greatly exceed the rate of polyaminoester hydrolysis anticipated for Poly 1. For this reason, we believe that ova, which is a relatively small and globular protein with low surface charge density, is able to readily diffuse out of

the Poly 1 films upon contact with aqueous solution, leading to a charge destabilization of the electrostatically assembled thin film and subsequent rapid dissolution of the film. Though the pH/ionic strength conditions used for PEM assembly here are near the buffer conditions used for analysis of rehydration and disassembly, our previous studies based on multilayer complexes of Poly-1 and anionic polysaccharides illustrated that subtle changes in solution pH can have dramatic effects on film disassembly kinetics.[19] The overall release kinetics were modestly altered by either using the more hydrophobic poly(*β*-amino ester) (Poly-2) for film assembly, or by decreasing the ionic strength of the dipping solutions from 100 to 10 mM to reduce charge screening and increase electrostatic interactions between the polyions during assembly, resulting in more tightly-associated PEM films (Figure 1c). Although there are undoubtedly additional strategies that could be used to further regulate protein release from these films, for our initial studies we hypothesized that rapid film dissociation on rehydration could be potentially advantageous for allowing maximal delivery of antigen/adjuvant molecules into barrier-disrupted skin prior to sealing of the epidermis (discussed further below).

These basic characterization measurements were made for films on glass substrates, which may not be ideal for application on skin. However, as there is virtually no restriction in the choice of the substrate for LbL assembly, we next tested assembly of Poly-1/ova films on substrates that might be useful in skin patch formulation. We tested poly(dimethylsiloxane) (PDMS) as an elastomeric substrate that could form the basis of easily-handled macroscopic patches, exploiting its well-known utility in microcontact printing to achieve intimate contact between drug-loaded multilayers and the inhomogeneous surface structure of skin. As illustrated in Figure 1d, film assembly was readily achieved on flexible PDMS substrates, and incorporation of fluorescent ova (ova-Texas Red) was readily observed from the blue hue of multilayer films on the transparent rubber.

We next tested whether ova protein assembled into Poly-1 LbL films, dried, and then rehydrated and released into buffer remained intact and unaggregated by running both non-reducing SDS-PAGE (Figure S3) and native PAGE on supernatants taken from (Poly-1/ova)$_{40}$ films assembled at different pHs, dried, and then rehydrated in PBS for 30 min. As seen in Figure 1e, almost all of the ova released from poly-1 films existed as monomeric protein running at the same position as unmanipulated control ova solutions in PAGE gels, indicating that the structural integrity of ova was preserved during both integration into and subsequent release out of the films. Ova released from films did not show significant signs of aggregation either with itself or with released Poly-1, as indicated by the lack of protein detected at positions above the main band of free ova in the PAGE gels. Lack of aggregation or degradation in the released ova suggests that proteins can be incorporated into poly-1 LbL films, dried, and released in a native monomeric state on rehydration without irreversible complexation to the polycation component of the films, an important outcome for the bioactivity of therapeutics or for the correct elicitation of antibody responses for vaccine antigens.

To assess antigen penetration into skin from LbL multilayers, we employed a murine ear skin model often used for analysis of antigen delivery for epicutaneous vaccination.[45, 46] This site provides a clearly defined draining lymph node (the auricular node) for immunological analysis, and Langerhans cells (LCs) within the ear are readily visualized by microscopy, allowing direct observation of protein delivery to these dendritic cells in intact tissue. Importantly, despite differences between murine and human skin structure, murine studies have been remarkably predictive for human clinical trials.[32] In order for vaccine agents to reach viable immune cells in the epidermis or dermis, the stratum corneum (SC), the thin, nonliving, exterior lipid-rich barrier layer of the skin must be bypassed.[47] One approach to transcutaneous vaccination is to employ adjuvant compounds that disrupt the

integrity of the SC, such as cholera toxin derivatives or heat labile-enterotoxin from bacteria.[42, 43] A simple and safe alternative is to physically disrupt the SC. This can be achieved using an approach such as glue or tape-stripping, based on the repeated application and removal of adhesives on skin, a process shown to remove the outer 10 – 20 μm of the SC. This barrier disruption process is painless, highly effective in augmenting the transfer of macromolecules such as proteins or DNA into skin, and has been successfully utilized in human clinical trials.[46, 48–50] An additional advantage is that physical barrier disruption itself has been shown to trigger activation of keratinocytes and LCs in skin, providing some level of 'built-in' adjuvant response.[44–46, 49–52] We thus tested a model where the dorsal ears of anesthetized mice were tape-stripped followed by application of as-assembled, air-dried $(Poly\text{-}1/ova)_{40}$ films on either glass or PDMS substrates, fixed in place by surgical tape against the exposed ear skin, mimicking a common strategy used in skin vaccination studies[45, 46] (Figure 1a). Tape-stripping reproducibly removed significant portions of the SC but did not disrupt the viable epidermis, as assessed by histology (Figure S3).

To assess protein release from LbL films into tape-stripped skin, films carrying fluorescent ova were assembled on PDMS patch substrates and applied to tape-stripped ear skin of C57Bl/6 mice or transgenic MHC II-GFP mice, whose Langerhans cells express GFP-tagged MHC molecules and are thus intrinsically labeled in the tissue. For comparison, we applied gauze pads loaded with an equivalent amount of fluorescent ova in saline to tape-stripped skin, mimicking the approach typically taken in vaccine studies. Mice were euthanized 48 h later, the PDMS patch or gauze was removed, and the skin sites were examined by confocal microscopy. Optical sections revealed the penetration of ova released from LbL films into the epidermis down to depths where LCs reside, 10 – 15 μm below the surface of tape-stripped skin (Figure 2a–b; LCs are readily distinguished by their branched/dendritic morphology). In separate experiments using C57Bl/6 mice, LCs deep in the epidermis below the main front of skin-penetrating ova were observed with pockets of internalized ova (Figure 2c), indicating that the cells were able to take up the delivered protein antigen from their surroundings. At the 48 h time point, LCs were observed with less pronounced dendritic morphology and at deeper depths than seen in fresh skin explants, suggesting that the cells were activated and in the process of beginning their slow migration to lymph nodes - a process known occur over a few days.[53, 54] In contrast, ova solutions applied to tape-stripped skin showed much less protein accumulation in the skin, and LCs were present at depths and densities in the epidermis more reminiscent of untreated skin (Figure 2b).

Immune responses are initiated in lymph nodes, where antigen-bearing dendritic cells directly interact with T- and B-lymphocytes, and thus antigen delivery to the nodes is critical for primary immune responses. Transport of antigens from the skin to the local lymph nodes can occur through direct draining of antigen deposited into the skin via lymphatic vessels or by cell-mediated transport, where activated LCs or other dendritic cells internalizing antigen in the skin migrate to the lymph nodes. To determine whether protein antigen released from LbL films applied to skin was transported to draining lymph nodes, murine ears were tape-stripped and LbL films on glass substrates carrying Alexa-fluor-conjugated ova were applied to the skin using surgical tape. As before, we compared LbL films to skin treated with gauze loaded with an equivalent amount of ova in saline. After 48 h, the skin-draining auricular lymph nodes were excised, digested, and recovered leukocytes were stained with antibodies for flow cytometry analysis. At this time-point, ova fluorescence could be directly visualized within intact lymph node tissue at low magnification (Figure 3a). CD11c is generally regarded as a marker for dendritic cells while CD11b is used to mark cells of myeloid lineage including monocytes and macrophages. Murine LCs and other dendritic cells migrating from skin have been shown to express both CD11c and CD11b surface molecules.[55, 56] As illustrated in Figure 3b–c, protein transport to the lymph nodes was detected

following treatment with a $(Poly\text{-}1/ova)_{50}$ LbL patch, when examining both the total lymph node cell population as well as individual cell subsets. Though $CD11c^+CD11b^+$ dendritic cells make up only a few percent of the total lymph node cells (e.g., as shown in the CD11c vs. CD11b flow cytometry plot for ova^- cells), these cells were greatly preferentially enriched in the ova^+ cell population, with ~64% of ova^+ cells being of the $CD11c^+CD11b^+$ subset (Figure 3b). As shown in Figure 3c, ~14% of all $CD11c^+CD11b^+$ dendritic cells acquired fluorescent ova following LbL film release of ova into the skin. Compared to tape-stripped skin treated with ova solution, ~1.8-fold more DCs and 2-fold more macrophages were positive for ova in the draining lymph nodes following LbL film delivery of the protein. Ova^+CD11c^+ dendritic cells exhibited up-regulation of the cell-surface activation markers CD40, CD86, and MHC II compared to ova^- dendritic cells (Figure 3d), suggesting that antigen-bearing DCs originating from skin acquired a mature phenotype during migration to the draining lymph nodes, consistent with prior studies.[57, 58] Mature dendritic cells are poised to present antigen and provide the appropriate stimulation required to trigger T- and B-cell activation. Thus, protein antigen released into barrier-disrupted skin from LbL films is delivered to skin-draining lymph nodes, where it accumulates in mature dendritic cells.

An attractive property of multilayers for controlled drug release is the ability to load multiple components into multilayer films and potentially tune the release kinetics of these cargos separately via the architecture of the films.[19] To explore multi-component drug delivery in the context of a transcutaneous vaccine, we next assembled LbL films incorporating both a protein antigen and an adjuvant cargo. Adjuvants are compounds typically co-injected with vaccines to increase their potency, reduce the required antigen dosage for a protective response, and/or to elicit immune memory with an appropriate protective profile.[59] We tested the co-incorporation of ova antigen in LbL films with CpG DNAs, short single-stranded oligonucleotides that contain unmethylated CpG (Cytosine--phosphate diester--Guanine) sequences characteristic of bacterial DNA. CpG DNA oligos are ligands for Toll-like receptor-9 on dendritic cells and other innate immune cells, and are a potent adjuvant currently in clinical trials for a variety of vaccine and cancer immunotherapy applications.[60] Immunologically, adjuvant signals such as CpG trigger dendritic cell activation, which is accompanied by a downregulation of antigen internalization by these cells.[61] Thus, we hypothesized that for vaccination, films capable of releasing antigen coincident with or prior to adjuvant release would be attractive. Further, sustained adjuvant delivery (mediated in basic immunological studies by repeated injections) have been shown to help break tolerance to tumor antigens in the setting of cancer vaccines, and so the ability to release adjuvant molecules for a period of several days could be a second important opportunity for LbL vaccine films.[62]

To regulate the release of antigen and adjuvant in composite films containing ova and CpG, we explored different sequences of layering in order to determine the impact of film architecture on the loading and release kinetics for the two components. We were also interested in examining potential interactions between ova and CpG within the film structure. Using Poly-2 as a complementary polycation for the two polyanionic cargos, co-delivery films containing ova and CpG were constructed with several different architectures (Figure 4a): control films of ova (A) or CpG (E) alone with Poly-2, CpG layered on top of ova (B), alternating ova and CpG (C), or ova layered over CpG (D). In each case 20 bilayers of Poly-2/ova and Poly-2/CpG were included. AFM imaging of dried films (Figure 4b) showed that each film composition exhibits a distinct surface morphology: films containing ova were generally rougher than CpG-loaded films (mean rms roughness 31±3 nm for $(Poly\text{-}2/ova)_{20}$ films vs. 8.5±2 nm for $(Poly\text{-}2/CpG)_{20}$ films). As described earlier, the release characteristics of the ova films suggest a high degree of interdiffusion of ova within the film, and high concentrations of ova at the top surface, typical of interdiffusion growth

behavior.[63] The roughness of the surfaces of the ova films may be a result of this interdiffusion, and accumulation of ova protein in the top layers. Film structures A and D, that were both terminated with multiple Poly-2/ova bilayers, were quite similar in their rough surface topography, whereas film structures B and C were rougher than E (pure Poly-2/CpG) films even though each film terminated with a Poly-2/CpG bilayer. These results suggest the presence of ova near the surface in some substantial concentration in each of these two film architectures as well, and thus indicates the potential for interdiffusion of the adsorbing species during assembly. We postulate that ova is a more diffusive species within the LbL layers compared to the more densely charged CpG oligonucleotides, despite its larger molecular weight. It has been shown that charge density is a key controlling element in the ability of macromolecular species to diffuse within multilayer films.[20, 64, 65] The CpG-only films illustrate a more linear release over much more extended time frames that correspond well with surface hydrolysis of the multilayer films. This hypothesis is further supported by the release profiles collected in Figure 4c, showing rapid release of ova from films rehydrated in PBS for all film architectures, similar to the results observed for pure Poly-1/ova films. In contrast, a sustained release of CpG adjuvant over 3 days is observed in all cases. Although each film architecture was prepared with the same number of bilayers of ova or CpG, the total amount of each component within the final films varied significantly with film architecture. In earlier work we found that if an underlying multilayer system exhibits a high degree of interdiffusion during its construction, then a second set of multilayers assembled atop the first will often also exhibit interdiffusion into the pre-existing film[19]; this behavior provides opportunity for high loadings of both components via diffusion and trapping of excess molecules within the film. Notably, architecture “B” with ova deposited first under bilayers containing CpG, enabled the loading of large quantities of both components in the film, and exhibited attractive staggered release kinetics, with the majority of antigen rapidly released within 24 h while the CpG adjuvant exhibited sustained release over a period of ~3 days. Although further tuning of component loading and individual release kinetics can be readily envisioned by manipulation of film assembly conditions and the choice of polycation components, the staggered release of antigen and adjuvant presented here demonstrates the potential of this approach to vaccine and other drug cargo delivery.

Finally, we tested the ability of ova/CpG composite films coated on PDMS “patches” to deliver both antigen and adjuvant into tape-stripped murine ear skin. Similar to the experiments with Poly-1/ova films, multilayer-coated PDMS patches loaded with fluorescently-tagged ova and CpG (architecture “B”) were applied to ear skin of MHC-Class II-GFP mice for 48 h, then patches were removed and the skin sites were analyzed by confocal microscopy. Optical sections tracked the penetration of both labeled ova and CpG released from the film into the epidermis of tape-stripped skin down to 15 – 20 μm below the tape-stripped surface (Figure 5a). Colocalization of GFP^+ LCs with ova and CpG fluorescence (Figure 5b) were likewise observed, suggesting LCs internalized both penetrated antigen and adjuvant from their surroundings. Interestingly, at the 48 hr time-point LCs were detected at greater depths of 15 – 20 μm compared with films containing only ova, possibly reflecting the effect of CpG activating LCs and enhancing their migration toward lymphatics located deeper in the skin en route to regional lymph nodes. Similar results were observed for films with architecture “C”. Thus, erodible ultrathin films loaded with antigen and adjuvant compounds can deliver both components into skin, providing delivery to dendritic cells in the skin as required for the initiation of immune responses. Analysis of the immune response triggered by such multilayer-coated patches is currently underway and will be presented in due course.

CONCLUSIONS

In summary, we demonstrated here protein-loaded LbL-assembled films as platform materials for constructing skin vaccine or drug delivery patches. This study provides a proof-of-principle for the use of dry LbL films as skin vaccine patches, whereby films loaded are rehydrated *in situ* on barrier-disrupted skin, antigen and adjuvant are released into the epidermis where they are taken up by skin-resident dendritic cells, and antigen is transported to draining lymph nodes. The ability of multilayer films to incorporate protein that can be stored in a dry state prior to application and then released from rehydrated films in a non-aggregated/non-degraded state may allow extended storage/shelf life of vaccine formulations and address challenges in vaccine distribution in developing countries. The generality of LbL assembly suggests that a variety of antigen and adjuvant molecules should be readily incorporated into these films. In addition, the ability of multilayers to conformally coat substrates should allow this approach to be used in tandem with other techniques for breaching the stratum corneum, such as using microneedles coated with multilayer delivery films.[19] To make this platform truly generic for delivering a wide range of synthetic antigens and adjuvants, biodegradable nano-carriers might be embedded as delivery vehicles within LbL films, to segregate film assembly/release properties from the characteristics of individual antigens/adjuvant molecules – an examination of such strategies is the subject of ongoing studies.

METHODS

Materials

Poly(β-amino esters) were synthesized according to previous literature.[9] Alexa Fluor 488, Alexa Fluor 647 and Texas Red-conjugated ovalbumin, NuPAGE 10% Bis-Tris gels, 10% Tris-Glycine gels, and all PAGE reagents were purchased from Invitrogen (Eugene, OR). All antibodies, anti-mouse PE-I-A^b, anti-mouse APC-CD11c, anti-mouse PE-CD11b, anti-mouse PE-CD40, anti-mouse PE-CD86 were purchased from BD Biosciences (San Jose, CA). CpG oligonucleotides were purchased from Integrated DNA Technologies (Coralville, IA).

Film preparation

All LbL films were assembled with a modified programmable Carl Zeiss HMS DS50 slide stainer. Typically, films were constructed on a glass slide with approximate size of 1×2 in^2, which was treated in a plasma cleaner (Harrick Scientific Corp.) with O_2 plasma for 5 min prior to use. The substrate was then dipped into Poly-1 solution (2.0 mg/mL in 100 mM NaOAc buffer) for 10 min and followed by three sequential rinsing steps with pH-adjusted water for 1 min each. Then the substrate is dipped into ova solution (0.10 mg/mL in 100 mM NaOAc buffer) for 10 min and exposed to the same rinsing steps as described above. The PDMS substrate was initially coated with poly(allylamine hydrochloride) (50 mM, pH 7.5), followed by the same protocol to build $(Poly\text{-}1/ova)_n$ multilayer as described above. Co-delivery film of ova with CpG was constructed in a similar manner with CpG solution (0.10 mg/mL in 100 mM NaOAc buffer, pH 6, mixture of 10% TAMRA-labeled DNA)

Film characterization

Protein loading on the film was quantified by measuring the absorbance of protein within the film using a UV/Vis spectrophotometer (Varian Cary 600). Ova and CpG release from the film was followed by measuring the fluorescence spectra of released ova-AF 488, ova-AF 647, and TAMRA-CpG in PBS (Quantamaster Fluorimeter, PTI). Film thickness was measured with a Tencor P-10 Surface Profilometer. Non-reducing SDS PAGE and native PAGE were performed using NuPAGE 10% Bis-Tris gel and 10% Tris-Glycine gels

respectively. Samples were diluted in LDS sample buffer for SDS PAGE according to the manufacturer's instructions, heated to 90 °C for 2 min and ran using MES SDS running buffer at 200 V for 35 min. For native PAGE, samples were diluted in native sample buffer without heating and ran under native running buffer at 75 V for 2.5 h. Finally, gels were stained with a silver staining kit (Pierce Biotechnology, Rockford, IL) according to the manufacturer's instructions.

In vivo murine ear skin penetration

Animals were cared for in the USDA-inspected MIT Animal Facility under federal, state, local and NIH guidelines for animal care. Tape-stripping was performed on wild type C5BL/6J mice (Jackson Laboratories, Bar Harbor, ME) and MHC-Class II GFP mice (a gift from Professor Hidde Ploegh) immobilized under isofluorane anesthesia. Ears were hydrated briefly with PBS before being subjected to tape-stripping 10 times using cellophane adhesive tape (Office Depot invisible tape). Tape-stripped ears were subsequently swiped with PBS and pat dry before the application of LbL films (on their supporting substrates) onto the dorsal side. The application site was then sealed using Tegaderm and Nexcare medical tape (3M, Minneapolis, MN). Patches were kept on site for 2 days, following which mice were sacrificed and their ears excised. After removing the patches and rinsing with PBS, ears were split into dorsal and ventral halves. For wild type mice, the cartilage-free dorsal halves were immunostained overnight with anti-mouse PE-I-A^b (MHC-Class II) antibody (2 μg/mL) to mark the LCs present. The stained ear sheet was then mounted on a glass slide and 3D Z-section images were obtained on a Zeiss LSM 510 confocal microscope using a 63x objective to visualize the penetration into skin. Relative fluorescence was determined by using Metamorph imaging software to compute the integrated intensity of images taken at each depth. Values obtained were then normalized by the maximum value measured in the entire stack of images; for the case of LC fluorescence, background signal was also subtracted prior to normalization. Histological sections of intact and tape-stripped mouse ears were prepared by fixing ears with formalin for 20 h and embedding in paraffin. Sections were sliced and stained with haemotoxylin and eosin.

Analysis of cells in auricular LNs

Auricular LNs recovered from mice were digested in a cocktail of Liberase Blendzyme 2 (Roche Applied Sciences, Indianapolis, IN) (0.28 WU/mL) and DNase I (Sigma, St Louis, MO) (50 ng/mL) prepared in serum free RPMI with gentle shaking for 1 h at ambient temperature. EDTA (5 mM) was added to quench enzymatic activity and the suspension was allowed to settle for 10 min, following which the freed cells in suspension were aspirated from the remaining undigested tissue matrix. Recovered cells were rinsed once in PBS containing 1% BSA and EDTA (5 mM), then twice in PBS containing 1% BSA before resuspending them in flow cytometry buffer (1% BSA, 0.1% NaN_3 in Hank's balanced salt solution, pH 7.4) at 4 °C. The cells were blocked with anti CD 16/CD 32 antibody (10 μg/mL) for 10 min and then stained with fluorescent antibodies against surface markers for 20 min on ice, followed by three washes with flow cytometry buffer and addition of propidium iodide (PI) (1.25 μg/mL) for viability assessment. Stained cells were analyzed on a BD FACSCalibur flow cytometer.

Supplementary Material

Refer to Web version on PubMed Central for supplementary material.

Acknowledgments

We thank E. Horrigan for help with animal studies. We thank the Center for Material Science and Engineering and Institute for Soldier Nanotechnologies for access to their characterization facilities. This work is supported by Institute for Soldier Nanotechnologies. Xingfang Su acknowledges the financial support from the Agency for Science, Technology and Research, Singapore

REFERENCES AND NOTES

1. Decher G. Fuzzy nanoassemblies: Toward layered polymeric multicomposites. Science. 1997; 277(5330):1232–1237.
2. Hammond PT. Form and function in multilayer assembly: New applications at the nanoscale. Adv Mater. 2004; 16(15):1271–1293.
3. Tang ZY, Wang Y, Podsiadlo P, Kotov NA. Biomedical applications of layer-by-layer assembly: From biomimetics to tissue engineering. Adv Mater. 2006; 18(24):3203–3224.
4. Jewell CM, Lynn DM. Multilayered polyelectrolyte assemblies as platforms for the delivery of DNA and other nucleic acid-based therapeutics. Advanced Drug Delivery Reviews. 2008; 60(9): 979–999. [PubMed: 18395291]
5. Picart C. Polyelectrolyte multilayer films: From physico-chemical properties to the control of cellular processes. Current Medicinal Chemistry. 2008; 15(7):685–697. [PubMed: 18336282]
6. Wang Y, Angelatos AS, Caruso F. Template synthesis of nanostructured materials via layer-by-layer assembly. Chemistry of Materials. 2008; 20(3):848–858.
7. Lvov Y, Ariga K, Ichinose I, Kunitake T. Assembly of multicomponent protein films by means of electrostatic layer-by-layer adsorption. J Am Chem Soc. 1995; 117(22):6117–6123.
8. Lvov Y, Ariga K, Kunitake T. Layer-by-layer assembly of alternate protein polyion ultrathin films. Chemistry Letters. 1994; (12):2323–2326.
9. Onda M, Lvov Y, Ariga K, Kunitake T. Sequential actions of glucose oxidase and peroxidase in molecular films assembled by layer-by-layer alternate adsorption. Biotechnol Bioeng. 1996; 51(2): 163–7. [PubMed: 18624325]
10. Voegel JC, Decher G, Schaaf P. Polyelectrolyte multilayer films in the biotechnology field. Actualite Chimique. 2003; (11–12):30–38.
11. Thompson MT, Berg MC, Tobias IS, Rubner MF, Van Vliet KJ. Tuning compliance of nanoscale polyelectrolyte multilayers to modulate cell adhesion. Biomaterials. 2005; 26(34):6836–6845. [PubMed: 15972236]
12. Elbert DL, Herbert CB, Hubbell JA. Thin polymer layers formed by polyelectrolyte multilayer techniques on biological surfaces. Langmuir. 1999; 15(16):5355–5362.
13. Thierry B, Winnik FM, Merhi Y, Tabrizian M. Nanocoatings onto arteries via layer-by-layer deposition: Toward the in vivo repair of damaged blood vessels. J Am Chem Soc. 2003; 125(25): 7494–7495. [PubMed: 12812471]
14. Rajagopalan P, Shen CJ, Berthiaume F, Tilles AW, Toner M, Yarmush ML. Polyelectrolyte nano-scaffolds for the design of layered cellular Architectures. Tissue Engineering. 2006; 12(6):1553–1563. [PubMed: 16846351]
15. Krol S, del Guerra S, Grupillo M, Diaspro A, Gliozzi A, Marchetti P. Multilayer nanoencapsulation. New approach for immune protection of human pancreatic islets. Nano Letters. 2006; 6(9):1933–1939. [PubMed: 16968004]
16. Swiston AJ, Cheng C, Um SH, Irvine DJ, Cohen RE, Rubner MF. Surface Functionalization of Living Cells with Multilayer Patches. Nano Letters. 2008; 8(12):4446–4453. [PubMed: 19367972]
17. Wilson JT, Cui WX, Chaikof EL. Layer-by-layer assembly of a conformal nanothin PEG coating for intraportal islet transplantation. Nano Letters. 2008; 8(7):1940–1948. [PubMed: 18547122]
18. Wood KC, Boedicker JQ, Lynn DM, Hammon PT. Tunable drug release from hydrolytically degradable layer-by-layer thin films. Langmuir. 2005; 21(4):1603–1609. [PubMed: 15697314]
19. Wood KC, Chuang HF, Batten RD, Lynn DM, Hammond PT. Controlling interlayer diffusion to achieve sustained, multiagent delivery from layer-by-layer thin films. Proc Natl Acad Sci U S A. 2006; 103(27):10207–10212. [PubMed: 16801543]

20. Lynn DM. Peeling back the layers: Controlled erosion and triggered disassembly of multilayered polyelectrolyte thin films. Adv Mater. 2007; 19(23):4118–4130.
21. Macdonald M, Rodriguez NM, Smith R, Hammond PT. Release of a model protein from biodegradable self assembled films for surface delivery applications. J Control Release. 2008; 131(3):228–234. [PubMed: 18721835]
22. Jewell CM, Zhang JT, Fredin NJ, Lynn DM. Multilayered polyelectrolyte films promote the direct and localized delivery of DNA to cells. J Control Release. 2005; 106(1–2):214–223. [PubMed: 15979188]
23. Jessel N, Oulad-Abdeighani M, Meyer F, Lavalle P, Haikel Y, Schaaf P, Voegel JC. Multiple and time-scheduled in situ DNA delivery mediated by beta-cyclodextrin embedded in a polyelectrolyte multilayer. Proc Natl Acad Sci U S A. 2006; 103(23):8618–8621. [PubMed: 16735471]
24. Kim BS, Park SW, Hammond PT. Hydrogen-bonding layer-by-layer assembled biodegradable polymeric micelles as drug delivery vehicles from surfaces. Acs Nano. 2008; 2(2):386–392. [PubMed: 19206641]
25. Caruso F, Mohwald H. Protein multilayer formation on colloids through a stepwise self-assembly technique. J Am Chem Soc. 1999; 121(25):6039–6046.
26. Vazquez E, Dewitt DM, Hammond PT, Lynn DM. Construction of hydrolytically-degradable thin films via layer-by-layer deposition of degradable polyelectrolytes. J Am Chem Soc. 2002; 124(47):13992–13993. [PubMed: 12440887]
27. Kim BS, Smith RC, Poon ZY. Langmuir. 2009
28. Kim BS, Lee H, Min YH, Poon Z, Hammond PT. Hydrogen-bonded multilayer of pH-responsive polymeric micelles with tannic acid for surface drug delivery. Chemical Communications. 2009; (28):4194–4196. [PubMed: 19585018]
29. Mitragotri S. Immunization without needles. Nature Reviews Immunology. 2005; 5(12):905–916.
30. Prausnitz MR, Langer R. Transdermal drug delivery. Nature Biotechnology. 2008; 26(11):1261–1268.
31. Babiuk S, Baca-Estrada M, Babiuk LA, Ewen C, Foldvari M. Cutaneous vaccination: the skin as an immunologically active tissue and the challenge of antigen delivery. J Control Release. 2000; 66(2–3):199–214. [PubMed: 10742580]
32. Glenn GM, Kenney RT, Ellingsworth LR, Frech SA, Hammond SA, Zoeteweij JP. Transcutaneous immunization and immunostimulant strategies: capitalizing on the immunocompetence of the skin. Expert Rev Vaccines. 2003; 2:253–267. [PubMed: 12899576]
33. Warger T, Schild H, Rechtsteiner G. Initiation of adaptive immune responses by transcutaneous immunization. Immunol Lett. 2007; 109(1):13–20. [PubMed: 17320194]
34. Klimuk SK, Najar HM, Semple SC, Aslanian S, Dutz JP. Epicutaneous application of CpG oligodeoxynucleotides with peptide or protein antigen promotes the generation of CTL. Journal of Investigative Dermatology. 2004; 122(4):1042–1049. [PubMed: 15102096]
35. Inoue J, Yotsumoto S, Sakamoto T, Tsuchiya S, Aramaki Y. Changes in immune responses to antigen applied to tape-stripped skin with CpG-oligodeoxynucleotide in mice. J Control Release. 2005; 108(2–3):294–305. [PubMed: 16209897]
36. Ishii Y, Nakae T, SakaMoto F, Matsuo K, Quan YS, Kamiyama F, Fujita T, Yamamoto A, Nakagawa S, Okada N. A transcutaneous vaccination system using a hydrogel patch for viral and bacterial infection. J Control Release. 2008; 131(2):113–120. [PubMed: 18700159]
37. Lynn DM, Langer R. Degradable poly(beta-amino esters): Synthesis, characterization, and self-assembly with plasmid DNA. J Am Chem Soc. 2000; 122(44):10761–10768.
38. Akinc A, Anderson DG, Lynn DM, Langer R. Synthesis of poly(beta-amino ester)s optimized for highly effective gene delivery. Bioconjugate Chemistry. 2003; 14(5):979–988. [PubMed: 13129402]
39. Murthy N, Xu MC, Schuck S, Kunisawa J, Shastri N, Frechet JMJ. A macromolecular delivery vehicle for protein-based vaccines: Acid-degradable protein-loaded microgels. Proc Natl Acad Sci U S A. 2003; 100(9):4995–5000. [PubMed: 12704236]
40. Bonifaz LC, Bonnyay DP, Charalambous A, Darguste DI, Fujii SI, Soares H, Brimnes MK, Moltedo B, Moran TM, Steinman RM. In vivo targeting of antigens to maturing dendritic cells via

the DEC-205 receptor improves T cell vaccination. Journal of Experimental Medicine. 2004; 199(6):815–824. [PubMed: 15024047]

41. Reddy ST, van der Vlies AJ, Simeoni E, Angeli V, Randolph GJ, O'Neill CP, Lee LK, Swartz MA, Hubbell JA. Exploiting lymphatic transport and complement activation in nanoparticle vaccines. Nature Biotechnology. 2007; 25(10):1159–1164.
42. Glenn GM, Scharton-Kersten T, Vassell R, Matyas GR, Alving CR. Transcutaneous immunization with bacterial ADP-ribosylating exotoxins as antigens and adjuvants. Infect Immun. 1999; 67(3): 1100–1106. [PubMed: 10024549]
43. Scharton-Kersten T, Yu JM, Vassell R, O'Hagan D, Alving CR, Glenn GM. Transcutaneous immunization with bacterial ADP-ribosylating exotoxins, subunits, and unrelated adjuvants. Infect Immun. 2000; 68(9):5306–5313. [PubMed: 10948159]
44. Godefroy S, Peyre A, Garcia N, Muller S, Sesardic D, Partidos CD. Effect of skin barrier disruption on immune responses to topically applied cross-reacting material, CRM197 of diphtheria toxin. Infect Immun. 2005; 73(8):4803–4809. [PubMed: 16040993]
45. Kahlon R, Hu YX, Orteu CH, Kifayet A, Trudeau JD, Tan RS, Dutz JP. Optimization of epicutaneous immunization for the induction of CTL. Vaccine. 2003; 21(21–22):2890–2899. [PubMed: 12798632]
46. Strid J, Hourihane J, Kimber I, Callard R, Strobel S. Disruption of the stratum corneum allows potent epicutaneous immunization with protein antigens resulting in a dominant systemic Th2 response. European Journal of Immunology. 2004; 34(8):2100–2109. [PubMed: 15259007]
47. Bos JD, Meinardi M. The 500 Dalton rule for the skin penetration of chemical compounds and drugs. Experimental Dermatology. 2000; 9(3):165–169. [PubMed: 10839713]
48. Choi MJ, Maibach HI. Topical vaccination of DNA antigens: Topical delivery of DNA antigens. Skin Pharmacology and Applied Skin Physiology. 2003; 16(5):271–282. [PubMed: 12907832]
49. Yagi H, Hashizume H, Horibe T, Yoshinari Y, Hata M, Ohshima A, Ito T, Takigawa M, Shibaki A, Shimizu H, Seo N. Induction of therapeutically relevant cytotoxic T lymphocytes in humans by percutaneous peptide immunization. Cancer Res. 2006; 66(20):10136–10144. [PubMed: 17047078]
50. Vogt A, Mahe B, Costagliola D, Bonduelle O, Hadam S, Schaefer G, Schaefer H, Katlama C, Sterry W, Autran B, Blume-Peytavi U, Combadiere B. Transcutaneous anti-influenza vaccination promotes both CD4 and CD8 T cell immune responses in humans. J Immunol. 2008; 180(3):1482–1489. [PubMed: 18209043]
51. Seo N, Tokura Y, Nishijima T, Hashizume H, Furukawa F, Takigawa M. Percutaneous peptide immunization via corneum barrier-disrupted murine skin for experimental tumor immunoprophylaxis. Proc Natl Acad Sci U S A. 2000; 97(1):371–376. [PubMed: 10618425]
52. Nair S, McLaughlin C, Weizer A, Su Z, Boczkowski D, Dannull J, Vieweg J, Gilboa E. Injection of immature dendritic cells into adjuvant-treated skin obviates the need for ex vivo maturation. J Immunol. 2003; 171(11):6275–6282. [PubMed: 14634145]
53. Larsen CP, Steinman RM, Witmerpack M, Hankins DF, Morris PJ, Austyn JM. Migration and Maturation of Langerhans Cells in Skin Transplants and Explants. Journal of Experimental Medicine. 1990; 172(5):1483–1493. [PubMed: 2230654]
54. Stoitzner P, Holzmann S, McLellan AD, Ivarsson L, Stossel H, Kapp M, Kammerer U, Douillard P, Kampgen E, Koch F, Saeland S, Romani N. Visualization and characterization of migratory Langerhans cells in murine skin and lymph nodes by antibodies against Langerin/CD207. Journal of Investigative Dermatology. 2003; 120(2):266–274. [PubMed: 12542532]
55. Henri S, Vremec D, Kamath A, Waithman J, Williams S, Benoist C, Burnham K, Saeland S, Handman E, Shortman K. The dendritic cell populations of mouse lymph nodes. J Immunol. 2001; 167(2):741–748. [PubMed: 11441078]
56. Douillard P, Stoitzner P, Tripp CH, Clair-Moninot V, Ait-Yahia S, McLellan AD, Eggert A, Romani N, Saeland S. Mouse lymphoid tissue contains distinct subsets of Langerin/CD207+dendritic cells, only one of which represents epidermal-derived Langerhans cells. Journal of Investigative Dermatology. 2005; 125(5):983–994. [PubMed: 16297200]
57. Weinlich G, Heine M, Stossel H, Zanella M, Stoitzner P, Ortner U, Smolle J, Koch F, Sepp NT, Schuler G, Romani N. Entry into afferent lymphatics and maturation in situ of migrating murine

cutaneous dendritic cells. Journal of Investigative Dermatology. 1998; 110(4):441–448. [PubMed: 9540989]

58. Wilson NS, El-Sukkari D, Belz GT, Smith CM, Steptoe RJ, Heath WR, Shortman K, Villadangos JA. Most lymphoid organ dendritic cell types are phenotypically and functionally immature. Blood. 2003; 102(6):2187–2194. [PubMed: 12791652]
59. Guy B. The perfect mix: recent progress in adjuvant research. Nature Reviews Microbiology. 2007; 5(7):505–517.
60. Vollmer J, Krieg AM. Immunotherapeutic applications of CpG oligodeoxynucleotide TLR9 agonists. Advanced Drug Delivery Reviews. 2009; 61(3):195–204. [PubMed: 19211030]
61. Shortman K, Liu YJ. Mouse and human dendritic cell subtypes. Nature Reviews Immunology. 2002; 2(3):151–161.
62. Yang YP, Huang CT, Huang XP, Pardoll DM. Persistent Toll-like receptor signals are required for reversal of regulatory T cell-mediated CD8 tolerance. Nature Immunology. 2004; 5(5):508–515. [PubMed: 15064759]
63. Picart C, Mutterer J, Richert L, Luo Y, Prestwich GD, Schaaf P, Voegel JC, Lavalle P. Molecular basis for the explanation of the exponential growth of polyelectrolyte multilayers. Proc Natl Acad Sci U S A. 2002; 99(20):12531–12535. [PubMed: 12237412]
64. Zacharia NS, DeLongchamp DM, Modestino M, Hammond PT. Controlling diffusion and exchange in layer-by-layer assemblies. Macromolecules. 2007; 40(5):1598–1603.
65. Kharlampieva E, Ankner JF, Rubinstein M, Sukhishvili SA. pH-induced release of polyanions from multilayer films. Physical Review Letters. 2008; 100(12)

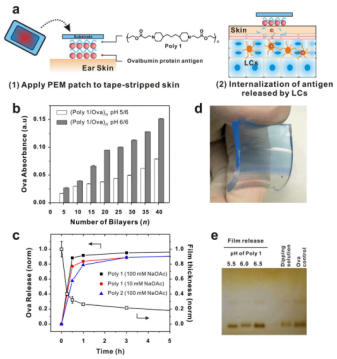

Figure 1.

(a) Schematic illustration of the events taking place following the application of PEM patch onto skin. (1) PEM patch on a substrate is applied onto tape-stripped ear skin. (2) Ova is released from the patch as the multilayer disassembles, and ova then penetrates to reach the LCs located at the basal layer of the epidermis. (b) Growth curve of (Poly-1/ova) multilayers for two different deposition conditions, as assessed by absorbance from fluorophore-conjugated ova incorporated in films. (c) Cumulative normalized kinetics of ova release from LBL films rehydrated in PBS (pH 7.4 at 25 °C), for films prepared with Poly-1 vs. Poly-2 and for Poly-1 deposition at low or high ionic strength. Representative thickness changes with time for a Poly-1/ova film assembled at high ionic strength. (d) Photograph of $(\text{Poly-1/ova-Texas Red})_{40}$ film assembled on a flexible PDMS substrate. (e) Native PAGE analysis of ova released from $(\text{Poly-1/ova})_{40}$ films after a 30 min rehydration in PBS, for films prepared by depositing ova at a fixed pH 6 and Poly-1 at pH 5.5, 6 or 6.5, respectively. Protein released from films is compared to controls of ova solutions in PBS pH 7.4 or in the multilayer deposition solution (pH 6,100 mM NaOAc buffer).

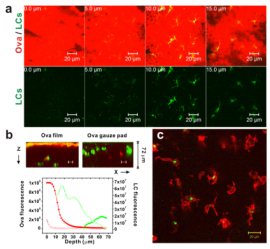

Figure 2.

(a) Overlay confocal micrographs (upper panel) taken at 5 μm intervals showing the penetration of Texas Red-conjugated ova (red) released from LbL films into tape-stripped ear skin of a MHC-Class II-GFP mouse following application of a Poly-1/ova PDMS patch for 48 h. Corresponding GFP fluorescence confocal micrographs (lower panel) showing Langerhans cells (LCs, green) appearing at *z*-depths of 10–15 μm below the tape-stripped skin surface, just above the epidermis-dermis boundary. (b) Representative vertical cross-sections and quantitative plots of fluorescence intensity normalized to maximum values for ova (red) and LC fluorescence (green) in skin treated with ova-loaded LbL films (filled symbols) or gauze pads with ova solution (open symbols). (c) Micrograph from an independent experiment, demonstrating colocalization of Alexa Fluor 488-conjugated ova (red) released from a Poly-1 LbL film and immunostained LCs (green) in the skin of a C57bl/6 mouse observed at a deeper depth where free ova in the surroundings is no longer detected, suggesting that activated LCs have taken up penetrated antigen and begun migration to lymph nodes. All scale bars are 20 μm.

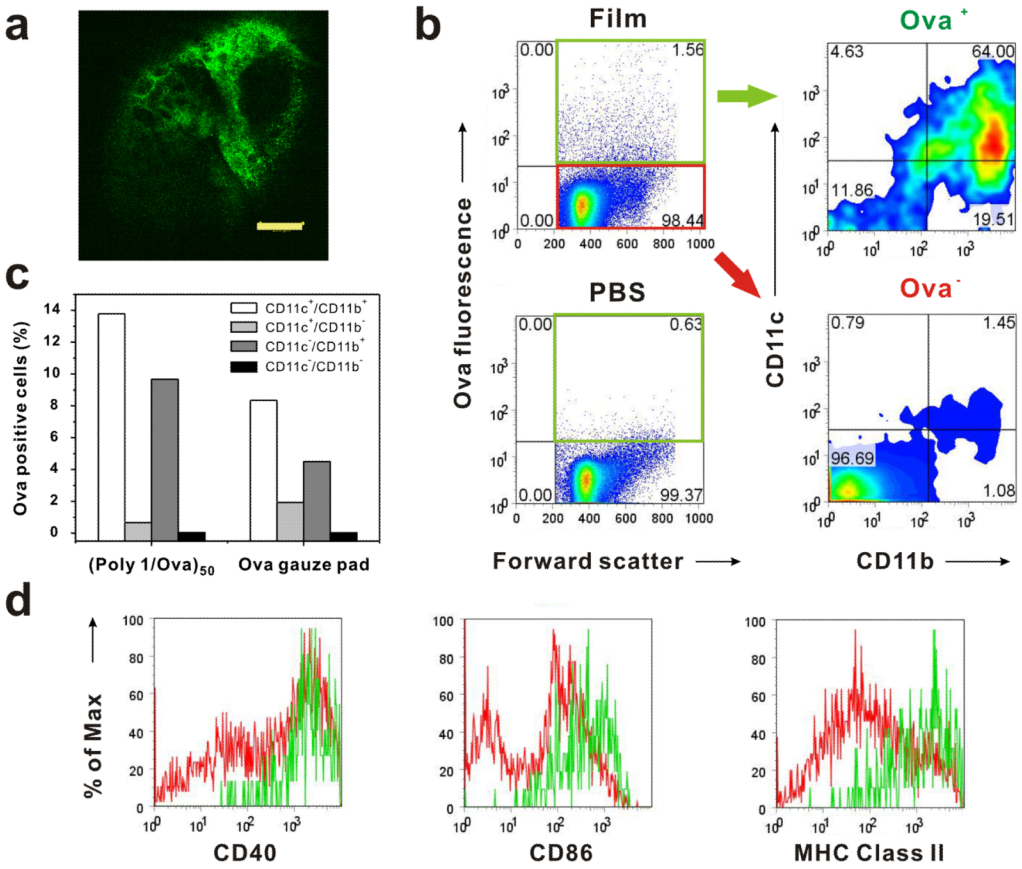

Figure 3.

(a) Confocal micrograph of intact auricular lymph node draining the ear site where ova-loaded LbL film was applied, showing ova fluorescence (green) accumulated in the tissue. (scale bar = 20 μm) (b) Left panels: Flow cytometry plots showing the proportion of total lymph node cells carrying ova (percentages quoted quadrant corners) as detected in the draining lymph node following skin treatment with ova-loaded LbL films or PBS as a control for 48 h. Right panels: Plots of CD11b vs. CD11c for ova$^+$ (green quadrant) and ova$^-$ (red quadrant) cells from the lymph nodes of mice treated with ova-loaded LbL films, showing that the majority of ova-bearing cells were CD11b$^+$CD11c$^+$ Langerhans cells and dendritic cells. (c) Percentages of ova$^+$ cells detected in macrophage and dendritic cell population subsets of skin-draining lymph nodes determined by staining recovered leukocytes for CD11c and CD11b surface markers. (d) Flow cytometry histograms of surface expression of costimulatory molecules CD40, CD86 and MHC-Class II by ova$^+$CD11c$^+$ dendritic cells (green line) and ova$^-$CD11c$^+$ dendritic cells (red line) recovered from lymph nodes of mice treated with ova-loaded LbL films.

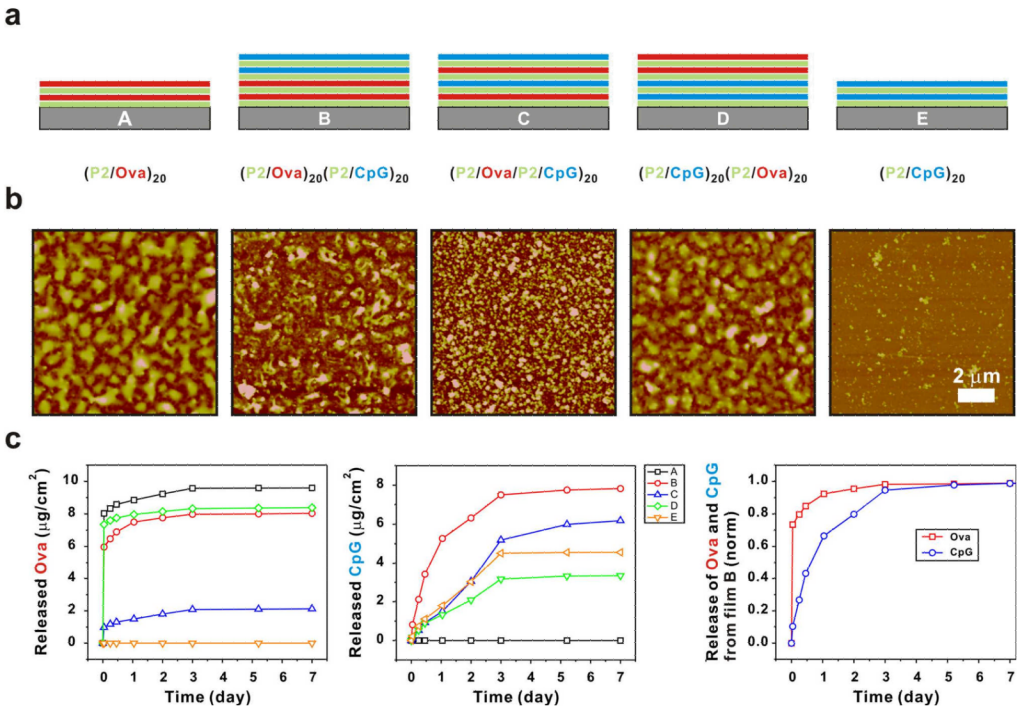

Figure 4.

(a) Schematic architectures of antigen (ova) and adjuvant (CpG DNA) co-delivery films tested. (b) AFM surface morphology of the corresponding dried films (10 × 10 μm^2 images, *z*-scale of 200 nm). (c) Kinetics of ova and CpG release from dried LbL films rehydrated in PBS (pH 7.4, 25 °C). Released ova and CpG were measured by collecting non-overlapping fluorescence signals ($\lambda_{max,Ova}$ = 665 nm, $\lambda_{max,CpG}$ = 560 nm), respectively. Overlay of normalized ova and CpG release curves from film architecture B.

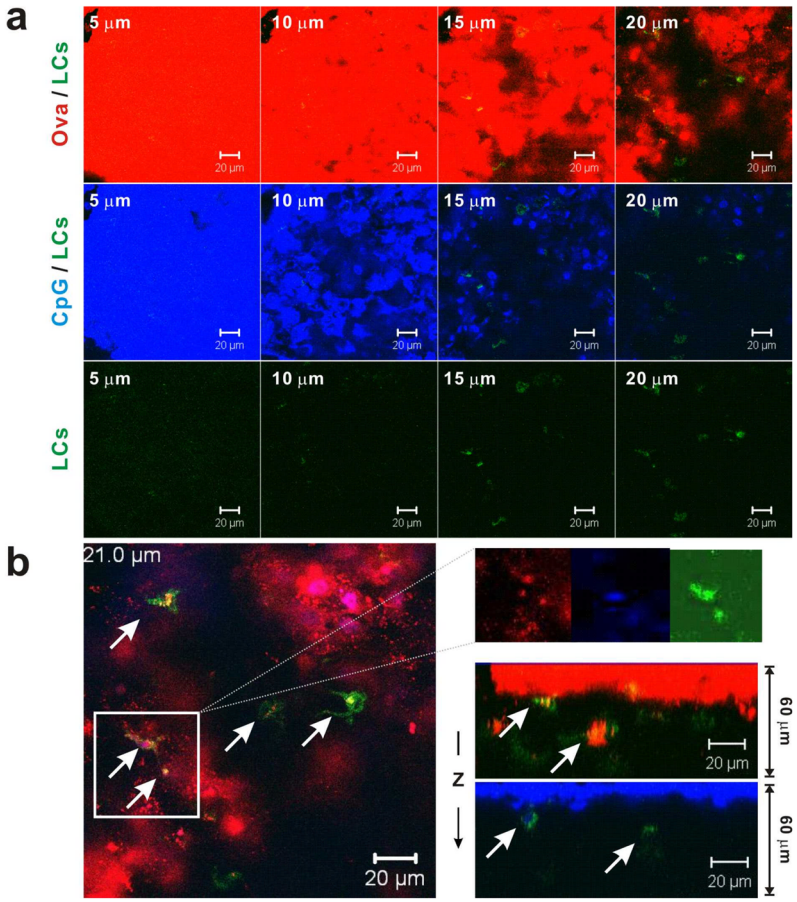

Figure 5.

(a) Overlay confocal micrographs (top and middle panels) taken at 5 μm *z*-intervals (*z*-depth indicated in upper left of each image) showing the penetration of fluorophore-conjugated ova (red) and CpG (blue) released from LbL films (architecture "B" from Figure 4a) into tape-stripped ear skin of MHC-Class II GFP mouse following patch application for 48 h. Corresponding GFP fluorescence confocal micrographs (bottom panel) showing LCs (green). (b) Representative horizontal (left) and vertical (lower right) cross sections showing colocalization of fluorescent ova and CpG with GFP^+ Langerhans cells (indicated by white arrows; inset figure shows individual fluorescent channel images of boxed region), suggesting uptake of penetrated antigen and adjuvant by the dendritic cells. Similar results were also observed for film architecture C (data not shown). Depths (below tape-stripped skin surface) of x-y confocal optical slices are noted (in μm) in upper left of micrographs. All scale bars 20 μm.